energies

MDPI

Article

Isobaric Expansion Engine Compressors: Thermodynamic Analysis of the Simplest Direct Vapor-Driven Compressors

Alexander Kronberg [1,*], Maxim Glushenkov [1], Sander Roosjen [2] and Sascha Kersten [2]

[1] Encontech B.V. TNW/SPT, P.O. Box 217, 7500 AE Enschede, The Netherlands; m.j.glouchenkov@utwente.nl
[2] Sustainable Process Technology, Faculty of Science and Technology, University of Twente, P.O. Box 217, 7500 AE Enschede, The Netherlands; s.roosjen@utwente.nl (S.R.); s.r.a.kersten@utwente.nl (S.K.)
* Correspondence: a.e.kronberg@utwente.nl

Abstract: Isobaric expansion (IE) technology is a promising solution for mini- and medium-scale low-grade heat utilization. IE engines directly convert heat to mechanical energy and are particularly interesting as direct-acting, vapor-driven pumps and compressors. The elimination of multiple energy transformations, technical simplicity and the ability to use widely available low-grade heat (<100 °C) instead of fossil fuels are attractive features of this technology. The purpose of this paper was to present a new compression technology based on IE Worthington type engines, analyze the process analytically and numerically, and provide a first assessment of its potential. The simplest single- and double-acting schemes were considered for arbitrary low and high pressures of the compressed gas/vapor and driving vapor. In these schemes, the compressor piston was rigidly connected to that of an engine/driver. The vapor use efficiency of the driver process was characterized by the ratio of the network carried out in the cycle to the consumed mass of the driving vapor. The performed thermodynamic analysis showed how the vapor use efficiency depends on the process parameters. It was found that the efficiency of vapor use in the simplest schemes was low in comparison with the efficiency in pumps if the compressor work was much less than the pump work at the same pressure ratio. This occurred because the energy of the driving vapor was spent on the compression of the vapor itself. As a result, the thermal efficiency of the IE engine compressors was lower than that of the IE engine pumps. The difference was very large if the work of the engine feed pump was significant and no heat regeneration is applied. The results obtained are very useful for achieving improvements in this interesting technology, which will be reported in subsequent publications.

Keywords: energy efficiency; heat-driven compressor; isobaric expansion engine; low-grade heat; piston compressor

Citation: Kronberg, A.; Glushenkov, M.; Roosjen, S.; Kersten, S. Isobaric Expansion Engine Compressors: Thermodynamic Analysis of the Simplest Direct Vapor-Driven Compressors. *Energies* **2022**, *15*, 5028. https://doi.org/10.3390/en15145028

Academic Editor: Alessia Arteconi

Received: 2 June 2022
Accepted: 5 July 2022
Published: 9 July 2022

1. Introduction

Today, Organic Rankine Cycle (ORC) technology is the unrivaled technical solution to the production of electricity (or the coproduction of electricity and heat) from a wide-ranging variety of energy sources [1]. However, the real contribution of ORCs to the world's electricity-generating capacity is very small. The total installed capacity of ORC plants is about 2.7 GW [2], i.e., 0.042% of the global electricity-generating capacity and 0.068% of the generating capacity based on thermal energy sources [3]. Such a marginal contribution of ORCs is mostly caused by economic reasons. ORC systems are too expensive, especially in the case of low-grade heat sources (<100 °C) and low power ranges [4–6].

Isobaric expansion (IE) technology [7] is a promising solution for mini- and medium-scale low-grade heat recovery and utilization. The IE process is an alternative to conventional gas/vapor expansion accompanied by a pressure decrease typical of all state-of-the-art heat engines. The essence of the process is that useful energy is generated at a high cycle pressure, whereas the rest of the cycle is performed at a low cycle pressure. As a

result, the engine design becomes simpler, and the contribution of thermal and mechanical losses into overall cycle efficiency can be much lower than in the conventional processes with expansion.

IE engines are the oldest types of heat engines. It will suffice to mention that Savery, Newcomen and Watt pumps fit into this group [8,9]. These machines were later replaced by more efficient well-known water steam expansion machines such as piston steam engines as well as steam turbines. Over the past few decades, many IE engines have been proposed and studied again under different names and for different applications [10–17]. The current status of the IE technology and important modifications to make IE machines competitive and cost-effective alternatives to state-of-the-art heat conversion technologies are presented in [7]. These systems are almost noiseless, can be fully balanced and have a very simple, reliable and inexpensive design. Some versions of the IE engines proposed in [7] avoid typical technical problems associated with well-known thermal-energy-driven systems, such as a failure of sealing components, lubrication and wear.

IE engines directly convert heat to mechanical energy in a very convenient hydraulic or pneumatic form that can be converted to any other form of energy. These engines look particularly attractive as vapor-driven pumps and compressors since the engines themselves operate as positive displacement pumps or compressors. In such applications, heat can be efficiently used for direct pumping and compression. This means that the intermediate generation of electricity, its transmission and further conversion back into mechanical power, which is typical of modern industry, is excluded.

The impact of these methods can be significant because they also allow the replacement of primary fossil energy sources with abundantly available low-grade heat, even at temperatures below 100 °C.

There are many potential applications of the proposed technology. IE compressors can replace conventional electrically driven compressors in all cases in which a low-grade heat source of sufficient capacity is available. The compression of air for energy storage systems and hydrogen, as well as air conditioning and vapor compression refrigeration, are examples of promising applications. Solar energy and waste heat from truck and ship diesel engines are ideal heat sources for vapor-driven compressors. In the future, such a source may be the waste heat of various fuel cells. All types of electrically driven compressors used today in refineries and chemical and food processing plants can in many cases also be replaced by compressors driven by multiple sources of waste heat, which are typical for such industries.

The theoretical and experimental results obtained with Worthington type IE engine pumps are very promising [18,19]. The engine can also work as a compressor. However, according to our knowledge, studies of such engines as compressors are almost completely missing in the literature.

Aphornratana and Sriveerakul proposed an interesting vapor compression system [20]. However, the system has not been evaluated properly. In particular, variations in the pressure in the system components were not taken into account in the force balance. Recent publications on this topic [21–23] do not distinguish between compression and pumping processes.

Steam/vapor-driven compressors are similar to direct-acting steam pumps, although the processes are different. They were used to actuate the air brakes of steam locomotives [24,25]. There are multiple patents on different steam/vapor-driven compressors [26–31]. However, to date, no application has been found for this compression technology.

The purpose of this paper was: (1) to present a new compression technology; (2) analyze the thermodynamics of the process analytically and numerically; (3) provide a first assessment of its potential. These topics represent the novelty of the present work.

It was found that the simplest, direct transfer of energy from driving vapor (working fluid of an engine) to compressed fluid is less efficient than that in vapor-driven pumps since the energy of the driving vapor is also spent on the compression of the vapor itself. In particular, for the given parameters of the driving vapor, its consumption is almost

independent of the useful work done. The results obtained might explain why the steam-driven compressors have not received further development or commercial success. On the other hand, and more importantly, these results are very useful for finding improvements in this interesting technology, which will be reported in subsequent publications.

2. Basic Schemes of Vapor-Driven Compressors

The two basic schemes of Worthington type IE single-acting and double-acting compressors shown in Figure 1 are similar to the Worthington type IE pump, although the processes are different. They consist of a compressor cylinder and a driver cylinder provided with pistons that are coupled by a connecting rod. The driver cylinder is equipped with vapor inlet/admission valve vd2 and outlet/exhaust valve vd1. Accordingly, the compressor cylinder has inlet/suction valve vc1 and outlet/discharge valve vc2. The inlet and outlet valves of the driver are forcedly actuated; the valves of the compressor are self-acting. In Figure 1, P_{cL} and P_{cH} represent the inlet/low and outlet/high pressures of the compressor; P_{dL} and P_{dH} refer to the outlet/low and inlet/high pressures of the driver.

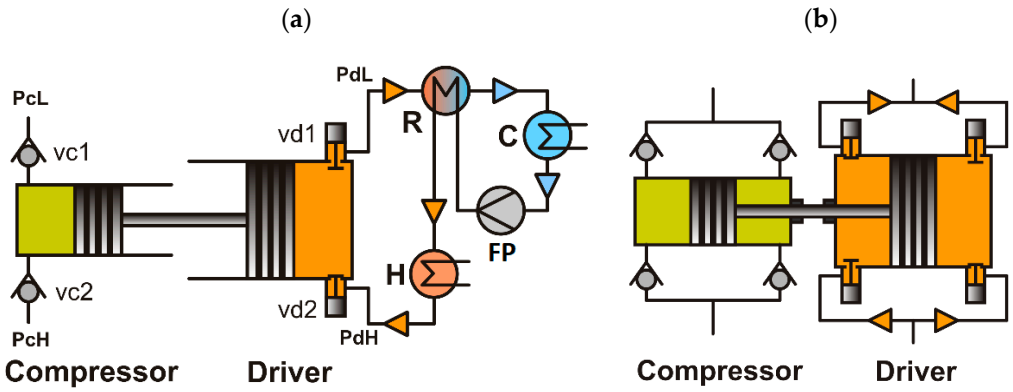

Figure 1. Basic schemes of vapor-driven compressors: (**a**)—single-acting, (**b**)—double-acting.

The driver cylinder is combined with a vapor generation circuit (shown in the single-acting scheme) consisting of a heater H, recuperator R, cooler C and feed pump FP. The driver together with the vapor circuit forms an IE heat engine. Its operation is described in [7,19].

The difference between the single-acting and double-acting compressors is in pressures acting on the pistons from different sides. In the case of the single-acting unit (Figure 1a), both the compression and actuation occur on one side of the compressor and driver pistons, and the pressures on the outer surfaces of the pistons are usually constant ambient pressures. In the double-acting type unit (Figure 1b), compression and actuation take place on both sides of the pistons, and the pressures on the outer surfaces of the pistons are the intake and discharge pressures of the compressor and driver, respectively.

The pistons are free in the sense that their movement is only controlled by the fluid forces acting upon them. The driver piston is actuated by a vapor generated in the vapor circuit. The reciprocating motion of the driver piston in each scheme is transformed into the reciprocating motion of the compressor piston.

The processes in the compressor and driver can be explained for the single-acting scheme, Figure 1a, as follows. Let us assume that initially, the compressor cylinder is filled with the compressed fluid at its intake or low pressure, P_{cL}, and the volume of the cylinder is maximal. During the compression step, the discharge valve of the driver vd1 is closed; the driving vapor is supplied to the driver through the intake valve vd2. The pressure of the driving vapor is transmitted through the driver piston and connecting rod to the compressor piston. During the compression step, the intake and discharge valves of the compressor are closed and pressure in the compressor increases from the initial/intake or low pressure, P_{cL}, to the final/discharge or high pressure, P_{cH}. Then, the compressed fluid under influence of the driving vapor at its maximum pressure, P_{dH}, is discharged

from the compressor through the outlet check valve vc2 at constant high pressure, P_{cH}. After that, the inlet valve of the driver vd2 closes, the outlet valve vd1 opens, and the pressure of the vapor in the driver drops from P_{dH} to the low driver pressure, P_{dL}. Due to change in the force acting on the pistons from the driving vapor side, they move a little to the right so that a small amount of the compressed fluid remaining in the compressor (mainly in the intake and discharge valves) expands and its pressure decreases to the intake pressure, P_{cL}; at the same time, part of the driving vapor is pushed out of the driver through the discharge valve vd1. After that, the compressor intake stroke begins, during which, pressure in the compressor remains constant, P_{cL}. Simultaneously, the rest of the driving vapor discharges from the cylinder through the valve vd1 at constant pressure, P_{dL}. At the end of the compressor intake and the driver discharge stroke, the system returns to the initial state, and the system is ready for the cycle to be repeated. The cycle period is controlled by the intake and discharge valves of the driver.

Figure 2a shows PV diagrams of the changes that occur in the cylinder of an ideal reciprocating compressor [32]. The corresponding pressure changes in the driver are presented in Figure 2b. Variables related to the driver and compressor are designated with indexes *d* and *c*, accordingly. In such a compressor and driver, resistances to the fluid flow in the inlet and outlet pipes and valves are negligible, and the fluid pressures during both the intake and discharge stages are constant.

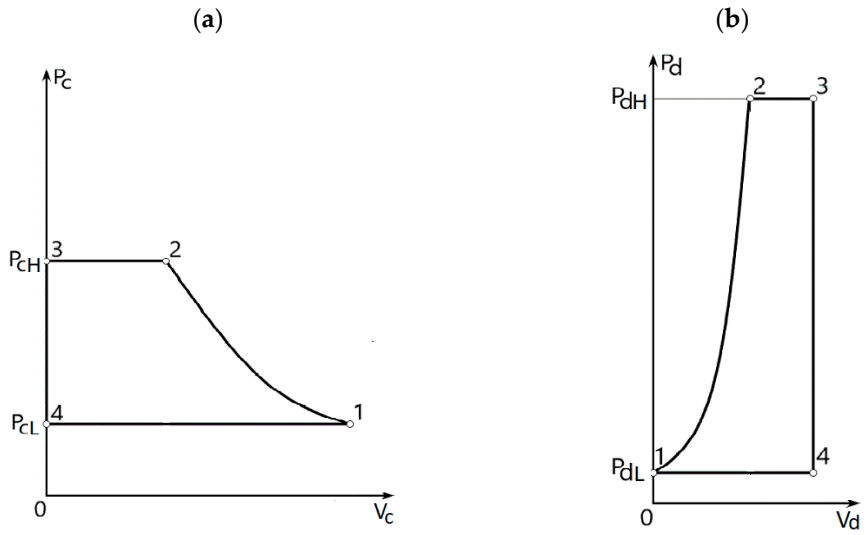

Figure 2. Pressure–volume change in the compressor (**a**) and driver (**b**) (indicator diagrams).

The diagram of the compressor, Figure 2a, assumes that when the piston has gone to the end of its stroke after compressing the sample of fluid, there is no fluid left in the cylinder between the piston and the seats of the discharge valve. This is referred to as an assumption of no clearance. The same assumption applies to the diagram of the driver, shown in Figure 2b. It is worth noting that points 3 and 4 in Figure 2a are both points of zero volume; the pressure difference is of no significance, and we can imagine the changes from 3 to 4 to occur instantly.

If the pistons move without acceleration (except the top and bottom dead centers), the pressure in the driver should correspond to the pressure in the compressor, as shown in Figure 2b. However, the change in the driving vapor pressure during the cycle can be different from the one shown in Figure 2b. It depends on the way the vapor is supplied to the driver.

As in the case of steam piston engines, the crucial issue is to find a method to supply the driving vapor to the driver, providing the highest amount of work. If the pistons of the compressor and driver are coupled by a mechanism such as a crank gear with a massive flywheel acting as energy storage, the solution is well known: a certain amount

of steam is to be injected at high pressure during an initial stage of piston movement, after which, the intake valve closes, and the supplied steam expands further adiabatically. However, this method would not be satisfactory in the case of the low mass of directly coupled pistons or low reciprocation frequency (around 1 Hz in IE engines) when inertia effects of the pistons and fluids are negligible. A large difference in the forces acting on the compressor and driver pistons, especially at the beginning of the compression stroke, leads to the uncontrollable acceleration of the piston pair, fluid to be compressed and excessive consumption of the driving vapor. Therefore, to avoid detrimental piston acceleration, the change in the driver pressure must match the variable pressure in the compressor, as shown in Figure 2.

An operation without acceleration (except the top and bottom dead points) will occur if the characteristic time of the pressure rise in the driver is lower than the characteristic time of the force equalization in the compressor and driver. Technically, this can be achieved by reducing the size of the intake driver valve for a given driver size. In addition, appropriate sizes of the compressor and driver pistons should be selected.

3. Relations between the Pressures and Piston Areas

For the single-acting compressor–driver combination, shown in Figure 1a, the relation between the pressures corresponding to the condition of the uniform piston movement is

$$(P_c - P_a)A_c = (P_d - P_a)A_d \tag{1}$$

where P_c and P_d are the pressures in the compressor and driver, A_c and A_d are the areas of the compressor and driver pistons and P_a is the ambient pressure.

To accomplish the compression, the maximum pressure of the driving vapor should be not lower than that obtained from the following equation:

$$(P_{cH} - P_a)A_c = (P_{dH} - P_a)A_d \tag{2}$$

For the intake stroke of the compressor, the discharge pressure of the driving vapor should not be higher than that obtained from the following equation:

$$(P_{cL} - P_a)A_c = (P_{dL} - P_a)A_d \tag{3}$$

From Equations (2) and (3), the ratio of the piston areas is

$$\frac{A_c}{A_d} = \frac{P_{dH} - P_{dL}}{P_{cH} - P_{cL}} \tag{4}$$

and the low and high pressures in the compressor and driver should obey the equation

$$\frac{P_{cH} - P_a}{P_{cL} - P_a} = \frac{P_{dH} - P_a}{P_{dL} - P_a} \tag{5}$$

Equation (5) places a severe restriction on the pressure range of the driver for given pressures in the compressor. In particular, for high-pressure processes, $P_{cL} \gg P_a$, $P_{dL} \gg P_a$, the ratios of the pressures in the compressor and driver should be the same. However, for many practically interesting applications, the compressor pressure ratio, $\frac{P_{cH}}{P_{cL}}$, is much higher than the driver pressure ratio, $\frac{P_{dH}}{P_{dL}}$, especially within the scope of the current research focused on the low-temperature difference applications of the IE engines. Therefore, the single-acting process scheme, shown in Figure 1a, is impractical since the choice of driving vapor pressures is limited.

The restrictions on the pressure of the driving vapor in the single-acting scheme, shown in Figure 1a, can be avoided using a modified, more flexible scheme, shown in Figure 3a. In this improved scheme, there is a large-volume receiver with a specified pressure, P_r, communicated with the second chamber of the driver or the compressor.

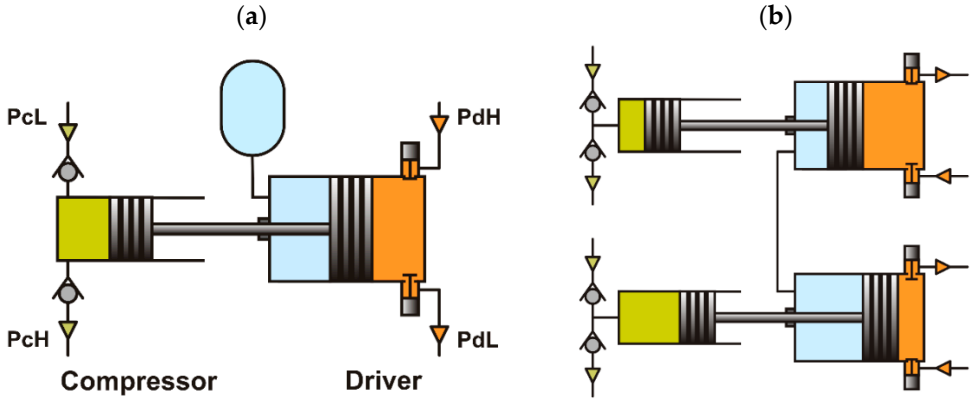

Figure 3. Modified single-acting schemes: with a receiver (**a**) and duplex scheme (**b**).

Applying the same reasoning as for the scheme without a receiver, the following equation relating the low and high pressure can be obtained, instead of Equation (5):

$$\frac{P_{cH} - P_a}{P_{cL} - P_a} = \frac{P_{dH} - P_r}{P_{dL} - P_r} \tag{6}$$

Pressure in the receiver, P_r, is an additional process parameter. Taking it as equal to

$$P_r = \frac{P_{dL}(P_{cH} - P_a) - P_{dH}(P_{cL} - P_a)}{P_{cH} - P_{cL}} \tag{7}$$

allows for any low and upper pressures to be used in the driver, P_{dL} and P_{dH}, for given values of low and upper pressures in the compressor, P_{cL} and P_{cH}. It can be shown that in this case, Equation (4) is also valid.

The scheme with the receiver, shown in Figure 3a, is a useful theoretical configuration. Better functionality can be achieved by using a duplex design, shown in Figure 3b. The duplex is a combination of two identical machines operating in counterphase, both auxiliary chambers of which (shown in blue in Figure 3b) are connected by a pipe. If the auxiliary chambers are filled with a gas at the pressure, P_r, needed in the receiver, they function as a large receiver without the compression/expansion of the gas inside them. The auxiliary chambers can also be used for lubrication, draining of working fluid leakages through seals, etc. Such an auxiliary chamber(s) can also be arranged in the compressor cylinder.

For the double-acting compressor–driver system, shown in Figure 1b, the forward and back strokes of the pistons are identical. In the case of a uniform piston motion, the relation between the pressures is:

$$(P_c - P_{cL})A_c = (P_d - P_{dL})A_d \tag{8}$$

Pressure in the compressor increases from P_{cL} to P_{cH} during the compression stroke and is constant, P_{cL}, during the intake stroke. Pressure in the driver changes in the range P_{dL}, P_{dH}. To accomplish the compression, the maximum pressure of the driving vapor, P_{dH}, should be not lower than the value from the equation:

$$(P_{cH} - P_{cL})A_c = (P_{dH} - P_{dL})A_d \tag{9}$$

from which the ratio of the piston areas is the same as for the single-acting unit, shown in Equation (4).

The pressure difference $P_{dH} - P_{dL}$ may be higher than that obtained from Equation (8). However, this is not justified. Excessively high driver pressure, P_{dH}, will cause unnecessary consumption of the driving vapor at the end of the compression stroke. Driver operation with an excessively low P_{dL} will require a controlled discharge valve to keep the driving vapor pressure at the level necessary for the uniform movement of the pistons.

A remarkable feature of the double-acting unit is that for any given value of low and high pressures in the compressor, P_{cL} and P_{cH}, arbitrary values of low and upper pressures in the driver, P_{dL} and P_{dH}, can be used.

Having in mind the modified single-acting schemes, shown in Figure 3, in the following analysis of the process efficiencies, there is no need to distinguish between single-acting and double-acting schemes. For any given pressures in the compressor, arbitrary low and high pressures in the driver can be applied.

4. Efficiency of Driving Vapor Use

The energy efficiency of the whole compression system is determined by the efficiencies of the compressor and driver as well as by the efficiency of the heat engine. In this paper, we focus on the efficiency of the driver. Its impact on the efficiency of the whole system is discussed separately.

In the subsequent analysis, we assume that the intake valve of the driver is open during the entire duration of the compression and discharge stages of the compressor so that pressure in the driver corresponds to the variable pressure in the compressor, as shown in Figure 2, and the pistons move without acceleration (except the top and bottom dead points).

The processes taking place in such systems are sufficiently complicated that idealizations are required to develop thermodynamic models, which represent an important initial step in engineering design. For simple analysis, the following usual assumptions are made [32]:

- The process in the compressor is either adiabatic or isothermal.
- The process in the driver is adiabatic.
- The driver only performs useful work on the compression.
- The minimum volumes of the compression and driving cylinder are zero (no dead volume).
- The temperature and pressure of the fluids in the driver and compressor are uniform.
- Mechanical friction between moving and stationary parts in contact (such as piston and cylinder, piston rod and stuffing box) is negligible.
- The inertia of the pistons, piston rods and the fluids is negligible; this is justified for IE engines operating at low frequencies.
- The cross-sectional area of the piston rods is much smaller than the area of the pistons.
- The heat capacities of ideal gases are constant.

In this and subsequent sections, most of the variables are related to the driver. Therefore, to simplify the notations, the index d, denoting the driver, is omitted. The subscript c is used to indicate compressor-related variables.

We assume that the driving vapor is delivered by the heat engine at pressure P_H and temperature T_H. This fluid is supplied to the driver through its intake valve serving as a throttle during the compression/forward stroke of the pistons involving the compression (compression stage 1–2) and displacement of the compressed fluid from the compressor (discharge stage 2–3); see Figure 2. After that, the discharge valve opens, the fluid is exhausted from the cylinder at constant volume, and the pressure of the driving vapor decreases to the low cycle pressure, P_L, and the fluid is discharged from the driver at this low pressure.

The driver process can be characterized by the ratio of the useful cycle work, W_c, to the consumed mass of the driving vapor, m_e, i.e., as the specific work:

$$w = \frac{W_c}{m_e} \tag{10}$$

In Equation (10), the useful work is designated as the cycle work of the compressor, $W_c = \oint P_c dV_c$, which is equal to the cycle work of the driver, $W = \oint PdV$, under the assumptions made. The mass of the consumed vapor is the mass of the vapor in the driver

at the end of the compression stroke. It depends on its temperature at the end of the compression stroke, T_e, and can be calculated as

$$m_e = \frac{V}{v(T_e, P_H)} \tag{11}$$

where V is the geometric chamber volume at the end of the compression stroke or the maximum driver volume and $v(T_e, P_H)$ is the vapor specific volume.

The specific work, w, can easily be calculated if the load on the driver piston is constant during the forward and back strokes of the piston. Such a constant load is realized in the limiting case when the compressor operates as an ideal pump. In this case, the driver performs the maximum possible work, $W_{max} = (P_H - P_L)V$, because the pressure of the driving vapor is maximal during the compression piston stroke and minimal during the discharge piston stroke. From the energy balance equation, it follows that the temperature of the driving vapor at the end of the compression/pumping stroke is T_H. Therefore, the vapor specific volume is $v(T_H, P_H)$ and the specific work of the driver operating as an actuator of the ideal pump is

$$w_p = \frac{W_{max}}{m_e} = (P_H - P_L)v(T_H, P_H) \tag{12}$$

w_p in Equation (12) is taken as the benchmark for the comparison of the efficiencies of the driver in this paper. Thus, the efficiency of driving vapor use can be defined as the relative specific work:

$$\alpha = \frac{w}{w_p} = z\frac{v(T_e, P_H)}{v(T_H, P_H)} \tag{13}$$

where

$$z = \frac{W}{(P_H - P_L)V} \tag{14}$$

is the relative work (or work ratio).

Since $W = W_c$ and $(P_H - P_L)V = (P_{cH} - P_{cL})V_c$ (see Equation (4)), z can be expressed as

$$z = \frac{W_c}{(P_{cH} - P_{cL})V_c} \tag{15}$$

α or T_e can be obtained from the energy balance for the compression stroke.

Assuming that the kinetic and potential energy contributions are negligible in comparison with the changes in internal energy and enthalpy, the unsteady-state macroscopic energy balance is

$$\frac{dmu}{dt} = h_{in}\dot{m}_{in} - h_{out}\dot{m}_{out} + \dot{Q} - \dot{W} \tag{16}$$

where m is the mass of the driving vapor, u and h are the specific internal energy and enthalpy, $\dot{m}$ is the mass rate of flow, $\dot{Q}$ is the net rate of heat addition to the system, and $\dot{W}$ is the net rate of work done by system on surroundings; indexes *in* and *out* refer to the inlet and outlet.

For the driver intake stroke, stages 1–2 and 2–3 in Figure 2b, $\dot{Q} = 0$, $\dot{m}_{out} = 0$. Since the enthalpy of the vapor does not change when it is released through a valve to a lower pressure (Joule–Thomson expansion), $h_{in} = h(T_H, p_H)$. Thus, Equation (16) for the driver intake stroke becomes

$$\frac{dmu}{dt} = h(T_H, p_H)\dot{m}_{in} - \dot{W} \tag{17}$$

Integrating Equation (17) from point 1 to point 3 (Figure 2b) gives

$$m_e u(T_e, P_H) = m_e h(T_H, P_H) - W_{13} \tag{18}$$

in which $T_e = T_3$ and $m_e = m_3$ are the temperature and mass of the vapor at the end of the compression stroke, represented by point 3 in Figure 2b, and W_{13} is the driver work in the compression stroke.

The net driver work in the cycle, W, which is equal to the cycle work of the compressor, W_c, is

$$W = W_c = W_{13} + W_{34} + W_{41} \tag{19}$$

where $W_{34} = 0$ and $W_{41} = -P_L V$ are the driver works in stages 3–4 and 4–1 (see Figure 2b), respectively.

Therefore, Equation (18) can be rewritten as

$$[h(T_H, P_H) - u(T_e, P_H)]m_e = W_c + P_L V \tag{20}$$

Substituting m_e from Equation (11) into Equation (20) we get

$$[h(T_H, P_H) - u(T_e, P_H)]\frac{V}{v(T_e, P_H)} = W_c + P_L V \tag{21}$$

If the compressor work, W_c, is known, T_e can be obtained from this equation. After that, all other characteristics of the process can be found. Equation (21) can readily be treated. The analysis is straightforward if the driving vapor is incompressible (e.g., water supplied under the constant head) or an ideal gas. For the incompressible driving vapor $\alpha = z$, i.e., the relative efficiency of vapor use is equal to the relative work.

4.1. Ideal Gases

In the case of an ideal gas enthalpy, internal energy, specific volume and specific heats are

$$h(T, P) = c_p T, \;\; u(T, P) = c_v T, \;\; v(T, P) = \frac{RT}{P} \tag{22}$$

$$c_p = \frac{R\gamma}{\gamma - 1}, \;\; c_v = \frac{R}{\gamma - 1}, \quad \gamma = \frac{c_p}{c_v} \tag{23}$$

in which R is the specific gas constant (the molar gas constant divided by the molar mass).

Combining these equations with Equations (15) and (21), the temperature of the driving gas at the end of the compression stroke (stage 1–3 in Figure 2b) and efficiency of the driving gas use, Equation (13), can be obtained:

$$\frac{T_H}{T_e} = 1 - \left(1 - \frac{1}{\gamma}\right)\left(1 - \frac{1}{r}\right)(1 - z) \tag{24}$$

$$\alpha = z\tau = \frac{z}{1 - \left(1 - \frac{1}{\gamma}\right)\left(1 - \frac{1}{r}\right)(1 - z)} \tag{25}$$

where $r = \frac{P_H}{P_L}$ is the driver pressure ratio and $\tau = \frac{T_e}{T_H}$ is the dimensionless temperature of the gas at the end of the end of the compression stroke.

Eliminating z from Equations (24) and (25), the relation between α and τ can be obtained:

$$\alpha = \frac{r}{r - 1}\left[\frac{\gamma}{\gamma - 1} - \left(\frac{1}{\gamma - 1} + \frac{1}{r}\right)\tau\right] \tag{26}$$

According to Equation (26), the efficiency decreases linearly with the dimensionless temperature of the driving gas at the end of the forward piston stroke, τ, expressed by Equation (24). Note that for compactness, Equation (24) represents $\frac{1}{\tau}$ as a function of the process parameters. According to this equation, $\tau = \frac{T_e}{T_H}$ increases with the driver pressure ratio, r, and the heat capacity ratio of the driving gas, γ, and decreases with the relative work, z. These trends are illustrated in Figure 4a. The lower the relative compression work, z, is, the higher the temperature of the driving gas at the end of the forward piston

stroke is. The opposite trend is found for the relative efficiency, α; see Equation (26) and Figure 4b. The greater the work performed by the driver, the higher the efficiency of the driving gas use.

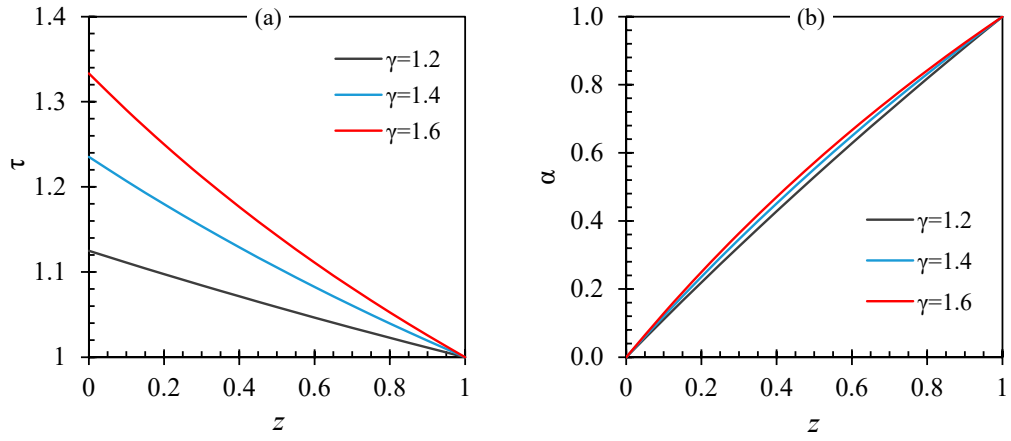

Figure 4. Dimensionless temperature of the driving gas at the end of the compression stroke (**a**) and relative efficiency (**b**) for different heat capacity ratios as a function of the relative work; r = 3.

If the driver performs the maximum possible work (equal to the ideal pumping work, z = 1), the temperature of the driving gas does not change, i.e., $\tau = 1$, and $\alpha = 1$, as follows from Equations (24) and (25). In the opposite case of negligible driver work compared to the maximum possible work ($z \ll 1$), the driving gas temperature approaches its maximal value, $\tau_{max} = \frac{\gamma r}{\gamma + r - 1}$ (for a given driving gas and driver pressure ratio), and the efficiency approaches zero; see Figure 4b.

Figure 5 shows the dimensionless temperature of the driving gas (a) and the gas use efficiency (b) as a function of the driver pressure ratio at $z = 0.5$. As the driver pressure ratio r approaches 1, the efficiency is not zero; however, the work done approaches zero.

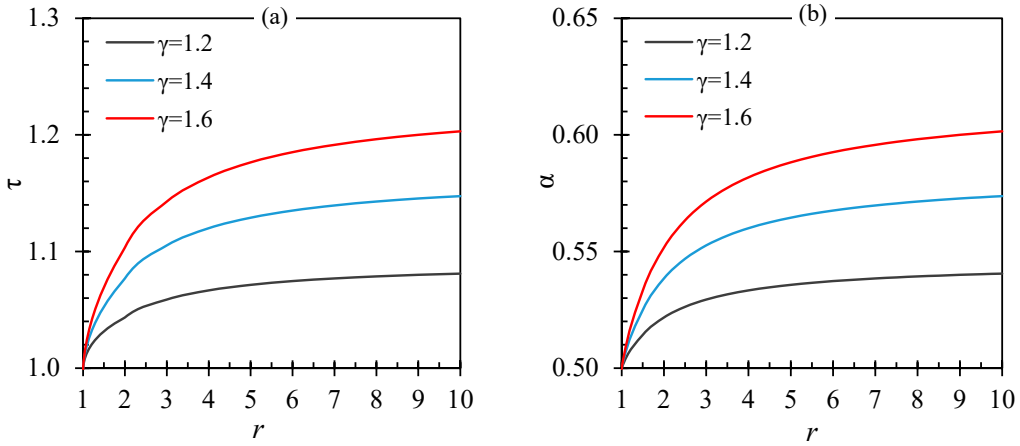

Figure 5. Dimensionless temperature of the driving gas at the end of the compression stroke (**a**) and relative efficiency (**b**) for different heat capacity ratios as a function of the driver pressure ratio; z = 0.5.

The results obtained clearly show that the relative work is the main factor that determines the efficiency of the driving gas use. The pressure ratio also affects the efficiency. However, if the relative work is small, no pressure ratio leads to a significant increase in the efficiency. Of the properties of a gas, only the ratio of heat capacities, γ, plays a role; it significantly influences the temperature of the gas if the relative work is small. The effect of γ on the efficiency appears at intermediate values of the relative work but disappears as z approaches 0 or 1.

The dependence of the efficiency on the parameters of the compressor process can be obtained using the expressions for the compressor work, W_c, in the equation for z; Equation (14). We study this dependence for two limiting compressor processes—adiabatic and isothermal compression.

In the case of adiabatic compression

$$W_{c,adiabatic} = P_{cL}V_c\frac{\gamma_c}{\gamma_c - 1}\left(r_c^{\frac{\gamma_c-1}{\gamma_c}} - 1\right) \quad (27)$$

and in the case of isothermal compression

$$W_{c,isothermal} = P_{cL}V_c ln(r_c) \quad (28)$$

where γ_c is the ratio of the heat capacities at constant pressure and constant volume of the compressed gas and $r_c = \frac{P_{cH}}{P_{cL}}$ is the compressor pressure ratio.

Figure 6 shows the calculated dimensionless temperature of the driving gas at the end of the piston stroke for the adiabatic and isothermal compression of an ideal gas and the efficiency of driving gas use as a function of the compressor pressure ratio.

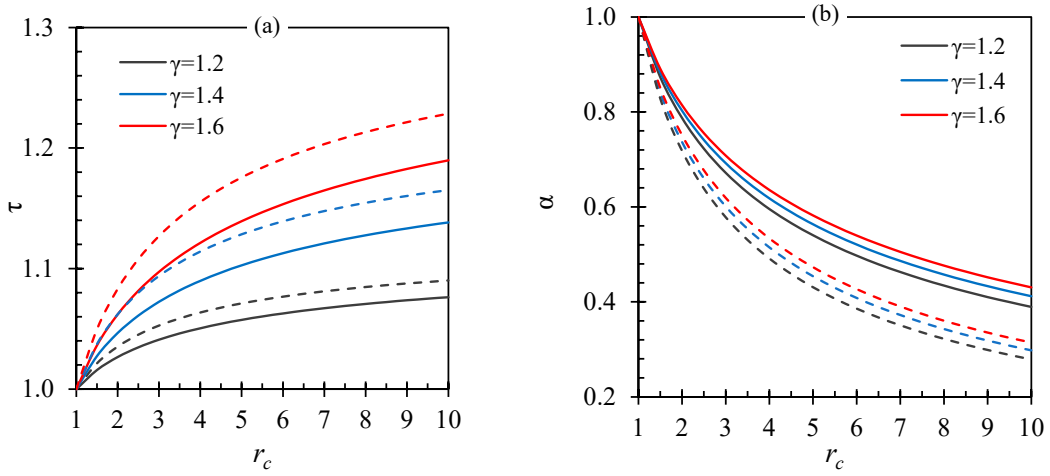

Figure 6. Dimensionless temperature of the driving gas at the end of the compression stroke (**a**) and efficiency of the driving gas use (**b**) as a function of the compressor pressure ratio and different γ; γ_c = 1.4, r = 3; solid lines—adiabatic compression, dashed lines—isothermal compression.

Figure 7 shows the results as a function of the driver pressure ratio. The relative position of the red, blue and gray lines in Figures 6a and 7a is explained by the fact that the temperature elevation of the driving gas with larger γ during the compression stroke is higher.

The results obtained show that the efficiency of the driving gas use for practically interesting compression processes (r_c is not close to 1) is significantly less than for pumping processes. This happens because the driving gas supplied to the driver cylinder compresses the compressed gas as well as the driving gas, which is already inside the driver. Accordingly, the consumption of the driving gas with higher γ is lower, whereas the efficiency of its use is higher.

The comparison of the isothermal and adiabatic compression processes shows that the temperature of the driving gas at the end of the compression stroke is higher for the isothermal compression; see Figures 6a and 7a. This means that the total amount of driving gas needed for the isothermal compression is less as the density decreases with temperature. Nevertheless, the work per unit mass of the driving gas is less in the case of an isothermal compression. Thus, an advantage of the isothermal compression compared to the adiabatic one is compromised by the inefficient use of driving gas.

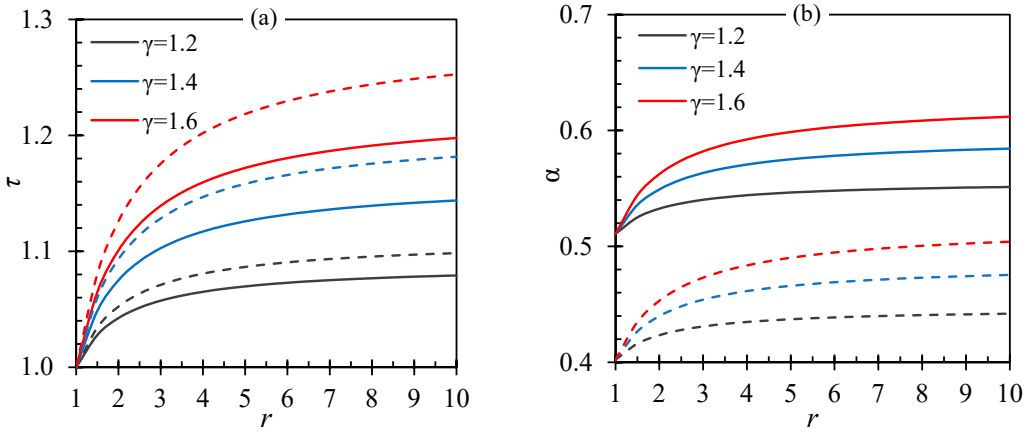

Figure 7. Dimensionless temperature of the driving gas at the end of the compression stroke (**a**) and efficiency of the driving gas use (**b**) as a function of the driver pressure ratio and different γ; γ_c = 1.4, r_c = 5; solid lines—adiabatic compression, dashed lines—isothermal compression.

The results obtained above for a driving vapor, which is an ideal gas, provide important qualitative conclusions about the performance of vapor-driven compressors. However, in real systems, the real gas effects can play an important role due to possible phase changes, especially when the IE engine is also considered as part of the system. Therefore, in the next section, the general analysis is extended to real gases used as driving and compressed fluids.

4.2. Real Gases

Equations (15) and (21) can be used to obtain efficiency α and temperature τ as a function of z, also when real gas is the driving vapor. Note that for these calculations, it is convenient to use the value of T_e as a parameter to obtain W_c and z as a function of T_e from Equations (15) and (21) and $\alpha(T_e)$ from Equation (13).

If the temperature change in the driving vapor is small, i.e., $T_e - T_H \ll T_H$, an approximate analytical solution can be obtained. Equation (21) can be rewritten as

$$[h(T_H, P_H) - h(T_e, P_H) + P_H v_e] \frac{V}{v(T_e, P_H)} = W_c + P_L V \tag{29}$$

Since the temperature difference $\Delta T = T_e - T_H$ is small, $h(T_e, P_H)$ can be expanded in a Taylor series around T_H, yielding

$$h(T_e, P_H) = h(T_H, P_H) + c_P(T_e - T_H) + O\left(\Delta T^2\right) \tag{30}$$

where $c_P = \left(\frac{\partial h}{\partial T}\right)_P$ and $O(\Delta T^2)$ designates terms of the second order of magnitude and higher and can be neglected.

At a small temperature difference:

$$T_e - T_H \approx \left(\frac{\partial T}{\partial v}\right)_P (v_e - v_H) = \frac{v_e - v_H}{v_H \beta} \tag{31}$$

where $v_e = v(T_e, P_H)$, $v_H = v(T_H, P_H)$, $\beta = \frac{1}{v}\left(\frac{\partial v}{\partial T}\right)_P$ is the isobaric expansion coefficient (or the volumetric thermal expansion coefficient at constant pressure).

Combining Equations (29)–(31) and using Equation (14), we obtain

$$\left[-\frac{c_P}{v_H \beta}(v_e - v_H) + P_H v_e\right] \frac{V}{v_e} = z(P_H - P_L)V + P_L V \tag{32}$$

From this equation

$$\frac{v_H}{v_e} = 1 - \frac{v_H \beta}{c_P}(P_H - P_L)(1 - z) \tag{33}$$

and the approximate expression for the efficiency, Equation (13), is

$$\alpha = z\frac{v_e}{v_H} = \frac{z}{1 - \frac{v_H \beta}{c_P}(P_H - P_L)(1 - z)} \tag{34}$$

The approximate temperature change can be obtained from Equations (31) and (33). In the case of an ideal gas

$$\frac{v_H}{v_e} = \frac{T_H}{T_e}, \quad v_H = \frac{RT_H}{P_H}, \quad c_P = \frac{R\gamma}{\gamma - 1}, \quad \beta = \frac{1}{T_H} \tag{35}$$

and Equations (31) and (34) transform to the exact Equations (24) and (25) derived above for ideal gases.

As an example of real gases, two well-known and widely used refrigerants—R134a (1,1,1,2-tetrafluoroethane) and R717 (ammonia)—were chosen as driving vapors. A reason for this choice is that both refrigerants are promising working fluids for IE engines in the low temperature range (<100 °C). The results on the engine pump efficiency for R134a are presented in [7,19,33]. Using the same approach as described in these papers, it was found that the efficiency of the ammonia cycle without heat regeneration for the low cycle temperature of 30 °C and the high cycle temperature in the range of 40–80 °C is 50–70% of the Carnot efficiency.

The chosen pressures and temperatures of the driving vapors are given in Table 1. These operating conditions are typical of IE engines [7]. The used discharge pressures of the R134a and ammonia of 7.7 bar and 10 bar correspond to their condensation temperatures of 30 and 25 °C, respectively. Fluid properties were taken from miniREFPROP 9.1 [34] and the NIST Chemistry WebBook, SRD 69 [35].

Table 1. Real gases and operating conditions of the driver.

Fluid	P_H (bar)	P_L (bar)	T_H (°C)	r
R134a	20 and 30	7.7	90	2.6 and 3.9
Ammonia	20 and 30	10.0	70	2 and 3

Figure 8 shows the calculated dimensionless temperature of R134a and ammonia at the end of the compression stroke (a) and the relative efficiency as a function of the relative work. Since the obtained efficiency, α, is approximately equal to the relative work, z, for better clarity, the dependence of α on z is presented as a dependence of $\alpha - z$ on z. The presented results were obtained using the numerical solution. Approximate analytical Equations (31), (33) and (34) give almost the same results; the difference is only a few percent.

The maximum values of $\alpha - z$ at $z \approx 0.5$ can be explained as follows: $\alpha - z$ is proportional to z and to $\frac{v_e}{v_H} - 1$; see Equation (34). If the temperature change is small, the specific volume change is also small; see Equation (31). From Equation (33), in this case, it can be shown that

$$\frac{v_e}{v_H} - 1 \approx \frac{v_H \beta}{c_P}(P_H - P_L)(1 - z) \tag{36}$$

Thus, $\alpha - z$ is proportional to $z(1 - z)$ which has a maximum at $z = 0.5$.

The comparison of Figure 8 with Figure 4, obtained for ideal gases, demonstrates the remarkable real gas effects. The values of temperature and efficiency for real gases, shown in Figure 8, do not correspond to those expected from the previous analysis of ideal gases. Table 2 presents the ratio of the heat capacities of R134a and ammonia for the process conditions.

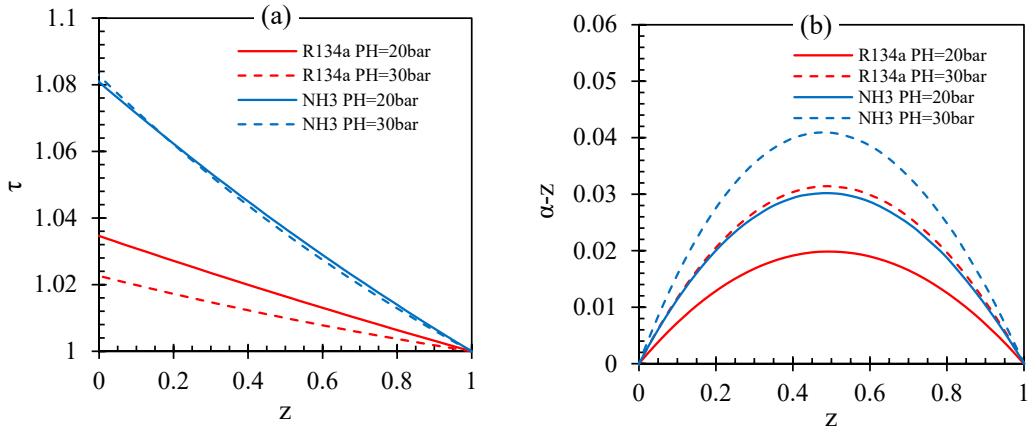

Figure 8. Temperature at the end of the compression stroke (a) and relative efficiency (b) for R134a and ammonia as a function of the relative work.

Table 2. Heat capacity ratios.

P_H (bar)	R134a			Ammonia		
	T_H (°C)	r	γ	T_H (°C)	r	γ
20	90	2.6	1.30	70	2	1.49
30	90	3.9	1.91	70	3	1.69

The heat capacity ratios of the refrigerants are quite high under process conditions; see Table 2. Therefore, based on the results obtained for ideal gases, shown in Figure 4a, a rather large temperature rise is expected. However, according to Figure 8a, R134a behaves as an ideal gas with γ = 1.05 and 1.03, and ammonia as an ideal gas with γ = 1.17 and 1.12 at P_H = 20 and 30 bar, respectively.

The results for ideal and real gases also differ qualitatively. Based on Equation (24) or Figure 5a for ideal gases, the temperature should increase with the increasing the pressure ratio, i.e., the blue lines ($P_H = 30$ bar) in Figure 8a are expected to be above the red lines ($P_H = 20$ bar). However, for ammonia, the temperature lines intersect, and the temperature of the R134a at $P_H = 20$ bar is higher than that at $P_H = 30$; Figure 8a. Based on Equation (25) and Figure 5b, the efficiency lines in Figure 8b should be located along the vertical axis in the same order as in Figure 8a. However, they are not.

A closer look at the energy balance and thermodynamic properties of the refrigerants under the process conditions explains the difference between the results obtained for real and ideal gases. The strong real gas effects are immediately apparent from the Pv values. For example, for R134a, $\mu Pv = \mu RT = 1760$ kJ/kmol at 90 °C and 20 bar, while for an ideal gas at the same temperature $\mu Pv = 3019$ kJ/kmol, where μ = 102.03 kg/kmol is the molar mass of R134a.

As an example of compressor processes, the adiabatic and isothermal compression of R134a and ammonia under conditions typical for refrigeration cycles for these refrigerants were considered. The operating conditions are presented in Table 3.

Table 3. Real gases and operating conditions of the compressor.

Fluid	P_{cL} (bar)	P_{cH} (bar)	T_{cL} (°C)	r_c
R134a	1	1–10	20	1–10
Ammonia	1	1–10	0	1–10

R134a and ammonia were also chosen as the driving vapors for the compression of R134a and ammonia, respectively. The driver operating conditions were taken to be the same as in previous examples; see Table 2.

To simplify the calculations, first, the temperature, τ, and efficiency, α, were calculated as a function of z, and then, the dependences of α on z and z on the compressor pressure ratio (obtained from the analysis of the compressor) were used to obtain the dependence of τ and α on the compressor pressure ratio.

Figure 9 shows the dimensionless temperatures of the driving refrigerants for the adiabatic and isothermal compression processes at different pressures of the driving vapor depending on the compressor pressure ratio. The obtained efficiency of the driving refrigerant use depending on the compressor pressure ratio is presented in Figure 10. In the case of isothermal compressions, the results are for the pressure ratio, r_c, below 5.7 for R134a and below 4.3 for ammonia at which the condensation of the vapors starts.

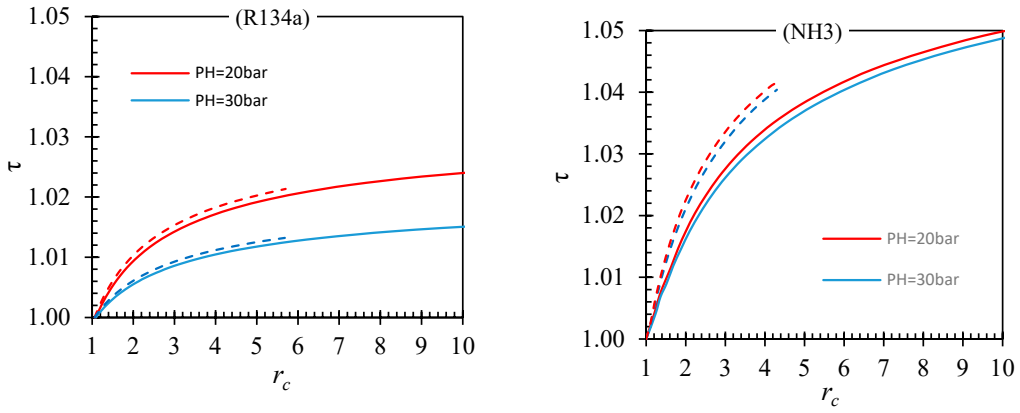

Figure 9. Dimensionless temperatures of the driving R134a (**left**) and ammonia (**right**) at the end of compression stroke as a function of the compressor pressure ratio; solid lines—adiabatic compression, dashed lines—isothermal compression.

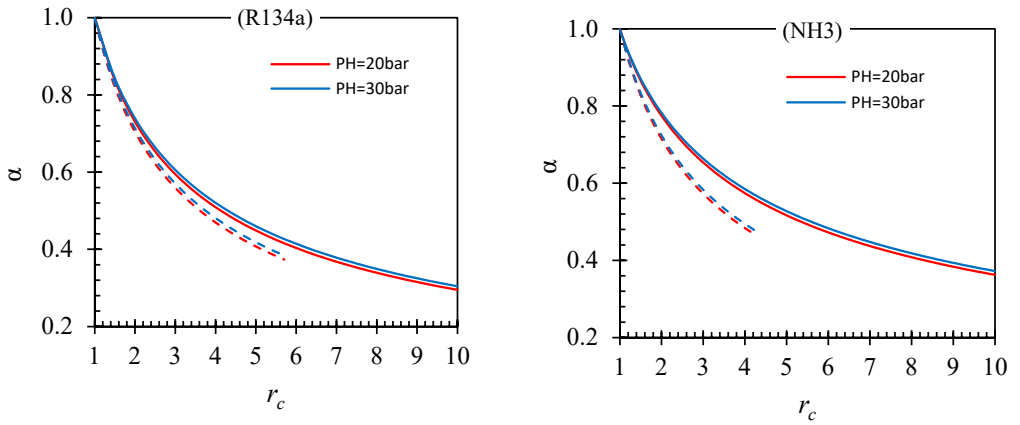

Figure 10. Efficiency of the driving R134a (**left**) and ammonia (**right**) use as a function of the compressor pressure ratio; solid lines—adiabatic compression, dashed lines—isothermal compression.

The relative work for compressing ammonia is higher than for R134a at the same pressure ratio. For example, with r_c = 5, the z value for ammonia compression is 0.489, and for R134a compression, it is 0.429. Due to the higher temperature and higher z, the efficiency of ammonia use for the compression of ammonia, shown in Figure 8b, is higher than the efficiency of R134a use for compression of R134a, shown in Figure 8a.

The influence of the driving vapor pressure is not pronounced for the considered pressures. There is practically no difference between the efficiencies at different pressures

of the driving vapor (blue and red lines in Figures 9 and 10). However, the compressor process, isothermal or adiabatic, has a strong influence on the efficiency of the driving vapor use (dashed and solid lines in Figure 10).

Comparing the results obtained for ideal gases, shown in Figure 6, and real gases, shown in Figures 9 and 10, it can be seen that behavior of the refrigerants in the driver is similar to ideal gases with a rather low ratio of the heat capacities, γ, of around or below 1.1.

However, due to strong real gas effects, predictions of the temperature and efficiency with the ideal gas equations are qualitatively different from those obtained for the real gases.

5. IE Engine Compressor Efficiency

The thermal efficiency of Worthington type IE engine, defined as the work done in relation to the heat supplied, can be presented in terms of specific works and enthalpies as [7]

$$\eta = \frac{w - w_{fp}}{\Delta h_{heater} - \Delta h_R} \tag{37}$$

where

$$w_{fp} = h\left(P_H, T_{fp,out}\right) - h(P_L, T_L) \tag{38}$$

is the work of the engine feed pump,

$$\Delta h_{heater} = h(P_H, T_H) - h(P_H, T_L) \tag{39}$$

is the heat absorbed/supplied in the heater and

$$\Delta h_R = h(P_H, T_L) - h(P_H, T_{R,out}) \tag{40}$$

is the regenerated heat.

In the equations above, T_L and T_H are the low and high engine cycle temperatures,$T_{R,out}$ is the temperature of the working fluid receiving heat at the outlet of the recuperator, and $T_{fp,out}$ is the discharge temperature of the engine feed pump which can be determined assuming an isentropic pump operation.

The work of the engine feed pump, w_{fp}, and the heat supplied in the heater, Δh_{heater}, do not depend on the compression process, whereas the regenerated heat is determined by the temperature of working fluid (driving vapor) discharged from the driver to the recuperator, which depends on its initial value, i.e., on the temperature of the driving vapor at the end of the compression stroke.

The efficiencies of the engine operating as compressor and pump can easily be compared for engines without recuperators (Δh_R = 0 in Equation (37)). The ratio of the efficiencies is:

$$\frac{\eta}{\eta_p} = \frac{w - w_{fp}}{w_p - w_{fp}} = \frac{\alpha - k}{1 - k} \tag{41}$$

in which $k = \frac{w_{fp}}{w_p}$ is the fraction of the feed pump work.

If the feed pump work is negligible, $\eta = \alpha\eta_p$. If the feed pump work cannot be neglected, the efficiency of the engine compressors decreases rapidly with increasing k and becomes zero as k approaches α.

The efficiency of the engine compressors will improve compared to that of the engine pump if heat regeneration is used since the temperature of the working fluid entering the recuperator from the driver is higher. This issue requires special consideration since the degree of heat regeneration largely depends on the properties of the working fluid [36].

6. Validation of the Engine Compressor Concept

In preparing this paper for publication, the first experimental studies were carried out to demonstrate that the compression technology under discussion is technically viable [37]. The scheme of the experimental setup, including the design of the compressor, is shown in Figure 11.

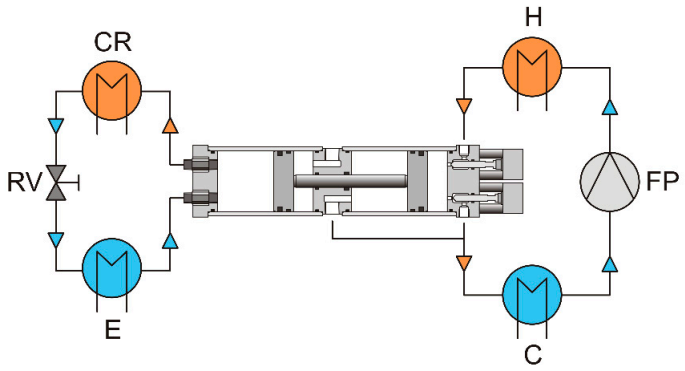

Figure 11. Scheme of the experimental setup.

The setup included the compressor itself and power and refrigeration loops. The power loop consisted of a heater (H), a piston feed pump (FP) and a cooler/condenser (C). The recuperator was not used in this scheme. The refrigeration/refrigeration loop consisted of a condenser (CR), an evaporator (E) and a control valve/throttle (RV).

All heat exchangers were brazed plate heat exchangers (SWEP). The regulating valve/throttle was a Swagelok metering needle valve. The IE compressor had two cylinders with internal diameters of 80 mm; the piston stroke was 100 mm. The R134a refrigerant was used as the working fluid in both the power and refrigeration cycles.

The operation of the compressor is outlined above (Section 2). The engine compressor was heated with hot water in the temperature range 30–80 °C and cooled with tap water at around 15 °C. The compressed refrigerant vapor was further condensed in the condenser (CR) and then expanded as it passed through the regulating valve (RV). The two-phase refrigerant mixture was then fed to the evaporator (E); finally, the vapor generated in the evaporator was sucked in by the compressor, where it again was compressed and delivered to the condenser. The operating frequency was in the range of 0.3–1 Hz.

The minimum temperature obtained in the evaporator reached −14 °C, although the most stable operation was observed at a higher temperature (0–4 °C). When the temperature of the heat source was too low (below 40 °C), the R134a vapor pressure was not always sufficient to provide the back stroke of the compressor. In this case, another refrigerant with a higher vapor pressure is needed. A more complex and versatile double-acting configuration, shown in Figure 1b, eliminates this limitation. The use of a double-acting scheme allows the generation of very low temperatures with many different refrigerants using heat sources even at ultra-low temperatures.

7. Discussion and Conclusions

In this paper, a new compression technology based on IE Worthington type engines was presented. Both the simplest single- and double-acting compression schemes were considered. The double-acting vapor compression scheme has an advantage over the single-acting one because the process can be arranged for any pressures of the driving vapor and the fluid to be compressed. However, the modification of the single-acting scheme by adding a receiver makes these schemes equivalent from this point of view. At first glance, the double-acting machines seem more practicable. Nevertheless, the final choice depends on many factors such as temperature, sealing type, etc. For instance, the single-acting design allows the adjacent (auxiliary) driver chamber (shown in blue in Figure 3) to be used to lubricate seals. The receiver is certainly a disadvantage of the single-acting scheme. To avoid energy losses due to gas compression in the receiver, its volume must be very

large, which makes such a scheme impractical. However, the problem of a large receiver is solved by using the duplex design typical of Worthington pumps.

The study of the simplest vapor compression schemes allows us to draw important conclusions about how operating parameters affect their performance. This follows directly from the obtained exact analytical solutions for ideal gases and approximate analytical solutions for real gases, which provide comprehensive information about the process. Analytical solutions can also be used to test numerical solutions for more detailed models.

It was found that the main criterion that determines the vapor use efficiency is the driver or compressor work, which depends on the compressor pressure ratio and properties of the compressed fluid. From the results obtained, one can easily deduce that for given parameters of the driving vapor, its consumption is almost independent of the useful work done. Therefore, if the driver work being performed deviates greatly from the maximum possible work, the efficiency of the driving vapor use is relatively low compared to the efficiencies of vapor-driven pumps, where pressures in the pump and driver do not change during the pumping and back strokes of the pistons. The efficiency approaches zero at small values of the work done. The reason for the low efficiency is that the pressure in the driver rises during the compression stroke, and a significant fraction of the energy of the driving vapor is spent on the compression of the driving vapor which was already supplied to the driver, rather than on the useful work.

The results obtained for ideal and real gases also show how the efficiency of the driving vapor use depends on the properties of the driving vapor and driver pressure ratio. The efficiency increases with the heat capacity ratio of the driving vapor and the driver pressure ratio, as follows from Equations (25) and (34).

Without heat regeneration, the application of the simple schemes considered in this work is doubtful due to the low efficiency of the driver process. Only if the compressor pressure ratio is very low (not higher than 2) or the driving vapor is generated by using no-cost waste heat can the whole process be economical. With heat regeneration, the conclusion may change. However, the analysis of heat regeneration, which can be arranged in different ways, is not simple and requires special consideration.

It is worth explaining the difference between isothermal and adiabatic compressions. The obtained vapor use efficiency in isothermal compression is lower than in adiabatic compression; see Figures 6b, 7b and 10, i.e., the work of compression per unit of driving vapor in isothermal compression is less. However, the amount of driving vapor consumed during isothermal compression is less due to the higher driving vapor temperature at the end of the compression stroke; see Figures 6a, 7a and 9. Moreover, the higher temperature is favorable for heat regeneration. Therefore, isothermal vapor-driven compression can be preferable to adiabatic compression.

The thermodynamic analysis performed provides ultimate efficiencies corresponding to negligible thermal and mechanical loses. The influence of neglected factors (free volumes in the compressor and driver, heat exchange between the fluids and the walls and inertia and friction of the pistons) on the system performance can be easily investigated numerically using more advanced models. For the simple processes considered in this paper, such a refinement of the model is not of interest, since even without the mechanical and heat losses, the thermal efficiency for practically interesting conditions is rather low.

The results obtained might explain why the steam-driven compressors used in the past and patented later have not received further development or commercial success. On the other hand, and more importantly, these results are very useful for finding improvements in this interesting technology. For example, the inefficient self-compression of the driving vapor can be reduced or eliminated by using multistage compression or a transmission between the driver and the compressor pistons. Another option is to recover the energy of the driving vapor discharged from the driver. The inefficient use of the driving vapor manifests in its higher temperature during the compression stroke. A relatively high-temperature driving vapor at the end of the compression stroke offers potential for the more efficient regeneration of its energy.

The energy of the driving vapor can also be recovered in mechanical form by reusing vapor that is released from the driver.

In subsequent publications, we will present several methods of different technical complexities, which make it possible to significantly improve the efficiency of compressors based on IE engines.

Author Contributions: Conceptualization, M.G. and A.K.; Methodology, A.K. and S.K.; Software, A.K. and S.R.; Validation, S.R. and S.K.; Formal Analysis, A.K. and S.R.; Investigation, A.K. and M.G.; Resources, S.K.; Data Curation, A.K. and S.R.; Writing—Original Draft Preparation, A.K.; Writing—Review and Editing, S.K. and M.G.; Visualization, M.G. and S.R.; Supervision, S.K.; Project Administration, A.K.; Funding Acquisition, A.K and M.G. All authors have read and agreed to the published version of the manuscript.

Funding: This research was funded by NPRP grant No. NPRP11S-1231-170155 from the Qatar National Research Fund (a member of Qatar Foundation). The findings achieved herein are solely the responsibility of the authors.

Conflicts of Interest: The authors declare no conflict of interest.

Nomenclature

A	Cross-sectional area (m^2)
c_p	Heat capacity at constant pressure (J/kg K)
c_v	Heat capacity at constant volume (J/kg K)
h	Specific enthalpy (J/kg)
IE	Isobaric expansion
k	Fraction of the feed pump work
m	Mass of the driving vapor (kg)
$\dot{m}$	Mass rate of flow (kg/s)
P	Pressure (bar)
Q	Heat (J)
r	Pressure ratio
R	Specific gas constant (the molar gas constant divided by the molar mass) (J/K kg)
t	Time
T	Temperature (°C, K)
u	Specific internal energy (J/kg)
v	Specific volume (m^3/kg)
V	Volume (m^3)
W	Work (J)
w	Specific work (J/kg)
z	Work ratio

Greek Letters

α	Relative vapor use efficiency
β	Isobaric expansion coefficient
γ	Heat capacity ratio
η	Thermal efficiency
μ	Molar mass (kg/kmol)
τ	Dimensionless temperature of the driving vapor at the end of the compression stroke

Subscripts

a	Ambient
c	Compressor
d	Driver
e	End of the compression stroke
fp	Feed pump
H	High
L	Low
p	Ideal pump
r	Receiver
R	Recuperator

References

1. Macchi, E. *Theoretical Basis of the Organic Rankine Cycle, in Organic Rankine Cycle (ORC) Power Systems*; Elsevier: Amsterdam, The Netherlands, 2017.
2. Tartière, T.; Astolfi, M. A World Overview of the Organic Rankine Cycle Market. *Energy Procedia* **2017**, *129*, 2–9. [CrossRef]
3. Q3 2017: Global Power Markets at a Glance. Available online: https://www.power-technology.com/comment/q3-2017-global-power-markets-glance/ (accessed on 2 June 2022).
4. Quoilin, S.; van den Broek, M.; Declaye, S.; Dewallef, P.; Lemort, V. Techno-economic survey of Organic Rankine Cycle (ORC) systems. *Renew. Sustain. Energy Rev.* **2013**, *22*, 168–186. [CrossRef]
5. Tocci, L.; Pal, T.; Pesmazoglou, I.; Franchetti, B. Small Scale Organic Rankine Cycle (ORC): A Techno-Economic Review. *Energies* **2017**, *10*, 413. [CrossRef]
6. Lemmens, S. A perspective on cost and cost estimation techniques for organic Rankine cycle systems. In Proceedings of the 3rd International Seminar on ORC Power Systems, Brussels, Belgium, 12–14 October 2015.
7. Glushenkov, M.; Kronberg, A.; Knoke, T.; Kenig, E.Y. Isobaric Expansion Engines: New Opportunities in Energy Conversion for Heat Engines, Pumps and Compressors. *Energies* **2018**, *11*, 154. [CrossRef]
8. Van der Kooij, B. *The Invention of the Steam Engine*; University of Technology: Delft, The Netherlands, 2015.

9. Whitmore, M. Development of Coal-Fired Steam Technology in Britain. In *Encyclopedia of the Anthropocene*; Elsevier: Amsterdam, The Netherlands, 2018; pp. 285–305.
10. Delgado-Torres, A. Solar thermal heat engines for water pumping: An update. *Renew. Sustain. Energy Rev.* **2009**, *13*, 462–472. [CrossRef]
11. Date, A.; Akbarzadeh, A. Theoretical study of a new thermodynamic power cycle for thermal water pumping application and its prospects when coupled to a solar pond. *Appl. Therm. Eng.* **2013**, *58*, 511–521. [CrossRef]
12. Oyewunmi, O.A.; Kirmse, C.J.W.; Haslam, A.J.; Müller, E.A.; Markides, C.N. Working-fluid selection and performance investigation of a two-phase single-reciprocating-piston heat-conversion engine. *Appl. Energy* **2017**, *186*, 376–395. [CrossRef]
13. Kirmse, C.J.W.; Oyewunmi, O.A.; Taleb, A.I.; Haslam, A.J.; Markides, C.N. A two-phase single-reciprocating-piston heat conversion engine: Non-linear dynamic modelling. *Appl. Energy* **2017**, *186*, 359–375. [CrossRef]
14. Glushenkov, M.; Bhosale, R.; Kumar, A.; AlMomani, F.; Kronberg, A. Heat powered water pump for reverse osmosis desalination. In *Materials for Energy, Efficiency and Sustainability*; TechConnect Briefs; CRC Press: Boca Raton, FL, USA, 2016; pp. 201–204. ISBN 9780997511710. Available online: www.TechConnect.org (accessed on 2 June 2022).
15. Markides, C.N.; Smith, T.C.B. A dynamic model for the efficiency optimization of an oscillatory low grade heat engine. *Energy* **2011**, *36*, 6967–6980. [CrossRef]
16. Solanki, R.; Galindo, A.; Markides, C.N. Dynamic modelling of a two-phase thermofluidic oscillator for efficient low grade heat utilization: Effect of fluid inertia. *Appl. Energy* **2012**, *89*, 156–163. [CrossRef]
17. Glushenkov, M.; Kronberg, A. Regenerative Heat to Mechanical Energy Converter with Dense Working Fluid. In Proceedings of the 16th International Stirling Engine Conference, Bilbao, Spain, 24–26 September 2014; pp. 177–186.
18. Available online: https://www.chester-project.eu/news/ie-engine-pump-in-ects-laboratory-video (accessed on 2 June 2022).
19. Glushenkov, M.; Kronberg, A. Experimental study of an isobaric expansion engine-pump—Proof of concept. *Appl. Therm. Eng.* **2022**, *212*, 118521. [CrossRef]
20. Aphornratana, S.; Sriveerakul, T. Analysis of a combined Rankine–vapour–compression refrigeration cycle. *Energy Convers. Manag.* **2010**, *51*, 2557–2564. [CrossRef]
21. Sleiti, A.K. Isobaric Expansion Engines Powered by Low-Grade Heat-Working Fluid Performance and Selection Database for Power and Thermomechanical Refrigeration. *Energy Technol.* **2020**, *8*, 2020. [CrossRef]
22. Sleiti, A.K.; Al-Ammari, W.A.; Al-Khawaja, M. Analysis of Novel Regenerative Thermo-Mechanical Refrigeration System Integrated with Isobaric Engine. *J. Energy Resour. Technol. Trans. ASME* **2021**, *143*, 052103. [CrossRef]
23. Sleiti, A.K.; Al-Khawaja, M.; Al-Ammari, W.A. A combined thermo-mechanical refrigeration system with isobaric expander-compressor unit powered by low grade heat—Design and analysis. *Int. J. Refrig.* **2020**, *120*, 39–49. [CrossRef]
24. Gibbs, K. *The Steam Locomotive. An Engineering History*; Amberley Publishing: Stroud, UK, 2009; Volume 2013.
25. Wells, D. *How a Steam Locomotive Works*; Allan Publishing: Shepperton, UK, 2010.
26. Wear, W. Steam Engine Air Pump. U.S. Patent 825,950, 17 July 1906.
27. Barner, J. Fluid Compressing Apparatus. U.S. Patent 1,372,891, 22 March 1921.
28. Hoop, R. Refrigeration System. U.S. Patent 2,986,907, 6 June 1961.
29. Cassady, V. Automotive Air Conditioning Apparatus. U.S. Patent 3,823,573, 16 July 1974.
30. Shelton, S.; Robinson, G.J. Dual Loop Heat Pump System. U.S. Patent 3,988,901, 2 November 1976.
31. Rowley, C.A.; Gutierrez, H.M. Heat Actuated Heat Pump. U.S. Patent 4,779,427, 25 October 1988.
32. Dodge, B.F. *Chemical Engineering Thermodynamics*; McGraw-Hill: New York, NY, USA; London, UK, 1944.
33. Knoke, T.; Kenig, E.Y.; Kronberg, A.; Glushenkov, M. Model-based Analysis of Novel Heat Engines for Low-Temperature Heat Conversion. *Chem. Eng. Trans.* **2017**, *57*, 499–504.
34. Lemmon, E.W.; Huber, M.L.; McLinden, M.O. *miniREFPROP, an Abbreviated Version of NIST REFPROP*; NIST Standard Reference Database 23, Version 9.1; NIST: Gaithersburg, MD, USA, 2013.
35. NIST. Thermophysical Properties of Fluid Systems. 2018. Available online: https://webbook.nist.gov/chemistry/fluid/# (accessed on 2 June 2022).
36. Kronberg, A.; Glushenkov, M.; Knoke, T.; Kenig, E.Y. Theoretical limits on the heat regeneration degree. *Int. J. Heat Mass Transf.* **2020**, *161*, 1–10. [CrossRef]
37. Available online: http://www.encontech.nl/video/Encontech_IE-engine_Refrigerator.mp4 (accessed on 2 June 2022).